Proximal and Long-Range Alterations in Chromatin Structure Surrounding the Chinese Hamster Dihydrofolate Reductase Promoter†

Alexander Pemov,‡ Sergei Bavykin,‡ and Joyce L. Hamlin*,§

Engelhardt Institute of Molecular Biology, Moscow 117984, Russia, and Department of Biochemistry, School of Medicine, University of Virginia, Charlottesville, Virginia 22908

Received August 10, 1994; Revised Manuscript Received December 7, 1994®

ABSTRACT: The chromatin structure of the dihydrofolate reductase (DHFR) gene was examined by DNA/protein cross-linking, chemical DNA methylation, and micrococcal nuclease digestion. The 5′ promoter region of the gene displays two nucleosome-free zones (−550 to −300 and −150 to +100 bp relative to the ATG codon), each of which contains a number of micrococcal nuclease-hypersensitive sites. Regions upstream from the distal hypersensitive zone (−900 to −550 bp), downstream from the proximal hypersensitive zone (+100 to +400 bp), and between these two zones (−300 to −150 bp) appear either to be more than 80% histone-free or to contain histones whose globular domains have lost most of their contacts with DNA. Overall, a broad zone extending from −4300 to +4700 bp is altered relative to bulk chromatin, and within this region there are positioned nucleosomes and/or nucleosome-free zones in which the DNA appears to interact with a number of different non-histone proteins. By comparison, the chromatin in the 3′ end of the gene (including the right end of the 5th intron and the 6th exon) contains randomly positioned nucleosomes, and its structure is intermediate between that of the 5′ end of the gene and a downstream matrix attachment region that contains regularly organized chromatin. A 2.3 kb zone in the central part of the 5th intron reveals some features similar to the 5′ end of the gene, suggesting a hitherto unrecognized functional role.

Dihydrofolate reductase (DHFR) catalyzes the reduction of folic acid to dihydrofolate and, subsequently, to tetrahydrofolate. The products of these reactions are required in the biosynthesis of purines, thymidine, and glycine. The gene encoding this enzyme is constitutively expressed in all tissues. The DHFR genes from mouse, human, and Chinese hamster have been cloned, mapped, and partially sequenced (Azizkhan et al., 1986; Carothers et al., 1983; Chen et al., 1984; Crouse et al., 1985; Hamlin & Ma, 1990; McGrogan et al., 1985; Milbrandt et al., 1983; Mitchell et al., 1986; Nunberg et al., 1980; Yang et al., 1984). Each gene has six exons, and the sequences of the coding regions and the 3′ untranslated region up to the first polyadenylation site, as well as the positions of intron−exon boundaries, are highly conserved.

In the promoter region of the murine, Chinese hamster, and human genes, four highly conserved elements are arranged very similarly with respect to one another (Azizkhan et al., 1986; Chen et al., 1984; McGrogan et al., 1985; Mitchell et al., 1986). None of the three promoters has canonical TATA or CAAT boxes. Instead, each gene displays several potential Sp1 binding sites (GC boxes) lying both proximal and distal to the major DHFR transcription start sites (Azizkhan et al., 1986; Chen et al., 1984; Farnham et al., 1986; McGrogan et al., 1985; Mitchell et al., 1986). In the case of the murine DHFR gene, at least one of the GC boxes has been shown to be required for efficient gene expression (Dynan et al., 1986). Indeed, interaction of Sp1 with GC boxes is apparently required for the regulation of start site utilization by RNA polymerase II in these TATA-less promoters (Blake et al., 1990). Another protein factor has been identified (HIP1, for "Housekeeping Initiator Protein 1") that is apparently also necessary for specifying the position of transcription initiation and whose binding site is located directly at the transcription start site (Means & Farnham, 1990). Thus, a synthetic minimal promoter for the DHFR gene should contain at least one Sp1 binding site and one HIP1 site (Buermeyer et al., 1992). Additional sequence elements between −46 and the middle of the first intron also appear to influence transcriptional activity (Farnham & Means, 1990).

The DHFR promoter is considered to be bidirectional, since a divergently transcribed gene has been identified in murine, Chinese hamster, and human systems (Crouse et al., 1985; Fujii et al., 1992; Linton et al., 1989; Mitchell et al., 1986; Shimada et al., 1989; Smith et al., 1990). In the murine and Chinese hamster genes, these transcripts initiate at ∼−300 and −195 bp, respectively, relative to the start codon of the DHFR gene. The distal clusters of GC boxes mapping between −700 and −400 relative to the start codons of the DHFR genes are therefore incorporated into the bodies of the divergent genes (Crouse et al., 1985; Farnham & Schimke, 1986; Mitchell et al., 1986).

The chromatin structures of the DHFR genes from Chinese hamster and human sources have been investigated in previous studies (Azizkhan et al., 1986; Mitchell et al., 1986; Shimada et al., 1986). The human gene has been characterized most extensively. A 1.1 kb region encompassing the promoter is completely unmethylated and contains several strong DNaseI-hypersensitive sites (Shimada & Nienhuis,

† This work was supported by NIH Grant RO1 GM26108, by an NIH Fogarty International Research Collaboration Award, and by the Russian State Program, "Frontiers in Genetics".

* To whom correspondence should be addressed. (804) 924-5858.
‡ Engelhardt Institute of Molecular Biology.
§ University of Virginia School of Biochemistry.

® Abstract published in *Advance ACS Abstracts,* February 1, 1995.

0006-2960/95/0434-2381$09.00/0

1985; Shimada et al., 1986, 1987); in the remaining 30 kb of the gene, all CpG sites are methylated and no hypersensitive sites are discernible (Shimada & Nienhuis, 1985; Shimada et al., 1987). A detailed analysis of the promoter of the human gene also suggests that the normal nucleosome array that characterizes bulk chromatin is interrupted from −760 to +150 bp relative to the transcriptional start site and that several nuclear proteins bind to specific sites within this 900 bp region of nucleosome-free DNA (Shimada et al., 1986). The pattern of methylation and the arrangement of hypersensitive sites are very similar in HeLa cells bearing one copy of the DHFR gene and in a methotrexate-resistant human cell line containing 80 copies of the gene (Shimada & Nienhuis, 1985). It was also shown that a plasmid carrying a completely methylated human DHFR minigene became demethylated only in the promoter region after transfection and stable integration into the genome of CHO cells; furthermore, the arrangement of hypersensitive sites in the promoter of the integrated minigene was restored to that of the normal human gene in its natural chromosomal context (Shimada et al., 1987). Thus, formation of the characteristic chromatin structure in the promoter is an intrinsic property of the underlying nucleotide sequence (Shimada et al., 1987).

The chromatin configuration in the promoter of the Chinese hamster DHFR gene has been examined in two independent studies, employing methotrexate-resistant cell lines containing either 300 or 1000 amplified copies of the gene (Azizkhan et al., 1986; Mitchell et al., 1986). When probed with DNaseI, the promoter displayed several regions of hypersensitivity flanking a zone of relative resistance centered at about −200 relative to the ATG codon. This pattern of DNaseI hypersensitivity is somewhat similar to that observed in the human gene promoter (Shimada et al., 1986). A 1.1 kb region that includes the promoter of the CHO gene was shown to be severely undermethylated relative to the remainder of the gene (Mitchell et al., 1986).

In the present study, we have carried out a much more detailed analysis of the chromatin structure in the Chinese hamster DHFR gene. We have used micrococcal nuclease digestion as well as two other chemical methods that have not been used to study the DHFR locus in any system so far. Our data indicate that the chromatin in the 5′ flanking region of the gene is specifically rearranged not only in the promoter itself but, surprisingly, over a region that extends from −4.3 to +4.7 relative to the transcription start site. In contrast, the 6th exon and the 3′ half of the 5th intron display randomly distributed nucleosomes and an overall structure that resembles bulk chromatin. A 2.3 kb region in the central part of the 5th intron displays unusual features suggesting a functional role that was not previously suspected.

MATERIALS AND METHODS

Tissue Culture and Isolation of Nuclei. The CHOC 400 cell line was developed and maintained as previously described (Milbrandt et al., 1981). Nuclei were isolated from cells in mid-exponential growth as detailed in Azizkhan et al. (1986).

Histone−DNA Cross-Linking Experiments. Fixation of nuclei with formaldehyde, cross-linking of histones to DNA by the dimethyl sulfate (DMS) method, enrichment of cross-linked DNA−histone complexes, and two-dimensional (2-D) gel electrophoresis were performed as previously described (Bavykin et al., 1993). The exception is that 6% and 10% polyacrylamide gels (PAGE; acrylamide/methylenebis(acrylamide) ratio of 30:1) were used in both dimensions for concentrating and separating gels, respectively.

DNA Methylation Experiments. After fixation with formaldehyde and methylation with DMS as described (Bavykin et al., 1993), nuclei were lysed with 0.5 M Tris-HCl, pH 8.0, containing 1% sodium dodecyl sulfate (SDS) and were heated in the same buffer for 30 min at 95 °C to cleave DNA at methylated sites. After digestion of chromatin proteins with proteinase K (1 mg/mL) for 90 min at 37 °C, DNA fragments were subjected to electrophoresis in the presence of 7 M urea, using the buffer system and conditions described for the first dimension of 2-D electrophoresis (Bavykin et al., 1993).

Micrococcal Nuclease Studies. To determine nucleosomal repeat lengths, nuclei were suspended at a concentration of 5 mg of DNA/mL in 10 mM Tris-HCl/1 mM $CaCl_2$, pH 8.0, and were digested with 0.625 mg/mL micrococcal nuclease (Sigma) for 10 min at 37 °C. In indirect end-labeling experiments, the conditions for digestion of nuclei and DNA by micrococcal nuclease were chosen to cleave less than once per 10 kb of DNA. Nuclei were suspended at 5 mg of DNA/mL in 10 mM Tris-HCl/1 mM $CaCl_2$, pH 8.0, and were digested with 0.125 mg of micrococcal nuclease/mg of DNA for 0.5−2.5 min at 37 °C. Control genomic DNA was purified by a standard protocol (Maniatis et al., 1989) and was dissolved at 75 mg/mL in 10 mM Tris-HCl/4 mM $CaCl_2$, pH 8.0, and digested with 0.125 mg of micrococcal nuclease/mg of DNA for 0.5−2.5 min at 37 °C. Reactions were terminated by adjusting to 12.5 mM EDTA, and samples were subjected to proteinase K digestion (0.5 mg/mL at 37 °C for 1.5 h), pancreatic RNase treatment (0.2 mg/mL at 37 °C for 30 min), and phenol/chloroform extraction. The purified DNA (0.1 mg/mL) was digested with 1 unit/mL *Xba*I or *Hin*dIII at 37 °C for 12 h in the buffers recommended by the supplier (BRL). Digests were separated on 1.5% agarose gels poured and run in 40 mM Tris-HCl/5 mM sodium acetate/1.25 mM EDTA, pH 7.8. The values for the nucleosomal repeat were calculated according to Noll and Kornberg (1977).

Blotting and Hybridization. DNA fragments were transferred from acrylamide gels to GeneScreen Plus (Dupont/NEN Research Products) by electroblotting in 10 mM Tris-HCl/5 mM sodium acetate/0.5 mM EDTA, pH 7.8, in a Bio-Rad TransBlot transfer system at 12 V for 10 h at room temperature (constant voltage). Southern blotting and hybridization procedures were carried out as described earlier (Dijkwel & Hamlin, 1988).

2-D Gel Scanning. Quantitation of autoradiographic images was performed as follows. The X-ray films were first calibrated by spotting known amounts of [^{32}P]dCTP onto 1 × 1 cm Whatman filter paper squares, drying, and exposing the filters to X-ray film for an appropriate time interval. Measurement of the integration volume, v (where v is the sum of the optical density values in each point), was performed on a Molecular Dynamics 300A computing laser densitometer (Image Quant, version 2.0). The values of v/s and d/s were determined for each rectangle and were then plotted against one another [where d is the total number of disintegrations (dpm × time of film exposure) and s is the area of the rectangle].

After scanning the 2-D gel autoradiograms, the *V/S* value for each diagonal was determined. *D/S* was determined using the calibration curve. *D*, which is proportional to the actual DNA content in the diagonal, was calculated by multiplying *D/S* by the square of the diagonal, *S*. To distinguish between parameters for the scanning of calibration rectangles and the diagonals themselves, we have denoted the two parameters with small and capital letters, respectively. The data presented in Table 1 represent the averages of three scans for each autoradiograph (error = ±5%).

Probes and Labeling Procedures. Five probes were used in hybridization experiments: (1) 103CAT extends from −103 to −16 and contains the major transcription start site at −63 relative to the A in the ATG codon (Mitchell et al., 1986); (2) 1.3R1 corresponds to an *Eco*RI fragment extending from −925 bp to +395 bp and includes the bidirectional promoter region, the first exon, and the first intron of the gene; (3) EX is a 1.4 kb *Eco*RI/*Xba*I fragment from the left end of the 6th exon; (4) INT is a 1.2 kb *Eco*RI/*Xba*I fragment that derives from the central portion of the 5th intron; and (5) MAR is a 400 bp *Pvu*II/*Hin*fI fragment situated over a prominent matrix-attachment region in the replication initiation locus in the DHFR domain (Dijkwel & Hamlin, 1988) and lies 30 kb downstream from the 3′ end of the DHFR gene. Probes were resected from plasmids and were random-primed and labeled with [^{32}P]dCTP as previously described (Dijkwel et al., 1991).

The experiments presented in Figures 3, 4A, and 5 were performed twice in their entirety, and the results obtained in the two experiments were essentially indistinguishable.

RESULTS

All experiments were performed on nuclei isolated from the methotrexate-resistant cell line, CHOC 400. CHOC 400 cells contain ~1000 copies of the DHFR amplicon per diploid nucleus (Milbrandt et al., 1981). The predominant amplicon type is 240 kb in length, and the multiple amplicons are organized in alternating head-to-head and tail-to-tail arrays at three chromosomal sites (Looney & Hamlin, 1987; Ma et al., 1988; Milbrandt et al., 1981).

Four different parameters of chromatin organization in the DHFR gene were investigated: (1) histone−DNA interactions in a defined region as revealed by DMS-induced histone−DNA cross-linking; (2) accessibility of DNA, as measured by the efficiency of methylation of defined sequences by DMS; (3) nucleosomal organization and the length of nucleosomal repeats, as determined by micrococcal nuclease digestion; and (4) nucleosomal positioning and probable interaction of defined sequences with non-histone proteins, as detected by hypersensitivity or changed accessibility to micrococcal nuclease in chromatin as compared to naked DNA.

In each of these methods, nuclei were isolated and treated with one or the other reagent, and DNA fragments were separated electrophoretically either by one-dimensional or by two-dimensional (2-D) PAGE or on agarose, as indicated in the flow chart in Figure 1. DNA fragments were transferred to a membrane and hybridized with appropriate probes for different parts of the DHFR gene (see map in Figure 2). In the DNA−protein cross-linking and DNA methylation experiments, nuclei were first fixed with formaldehyde to prevent protein redistribution and loss from active chromatin regions, which may occur during subsequent manipulations (Bavykin et al., 1993). Since formaldehyde induces both protein−protein and DNA−protein cross-links, which would render specific protein−DNA complexes impossible to identify, the formaldehyde cross-links were reversed prior to electrophoretic analysis.

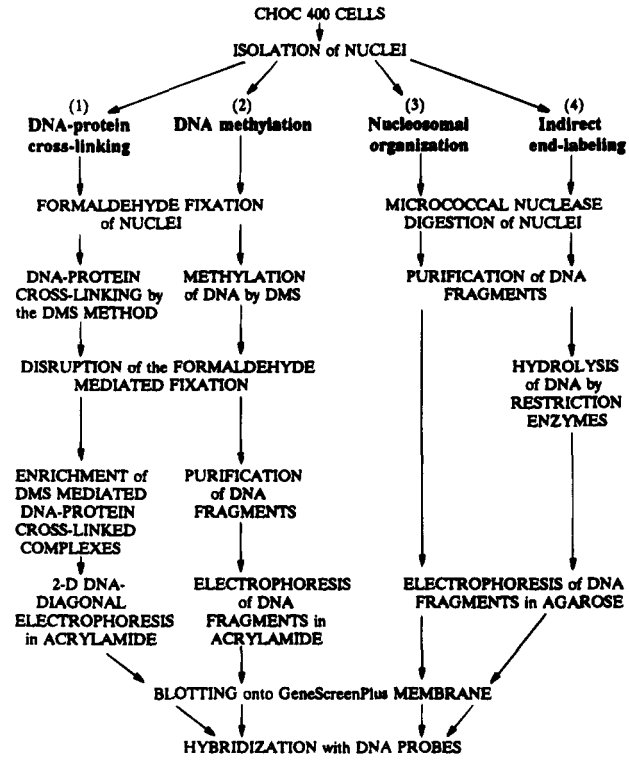

FIGURE 1: Flow chart of experimental procedures. For details, see Materials and Methods.

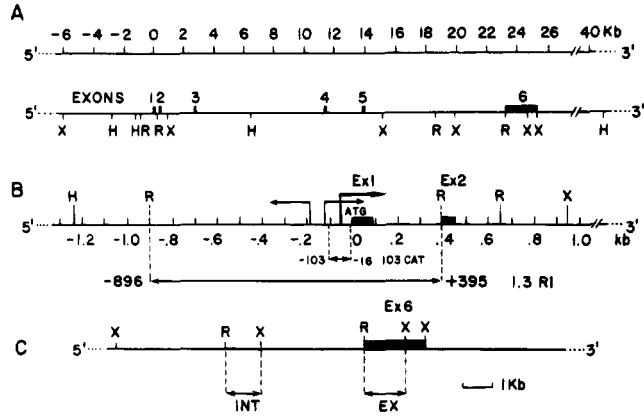

FIGURE 2: Maps of the CHO DHFR gene. Panel A: Map of the 26 kb DHFR gene and flanking regions, showing the positions of the six exons, as well as relevant *Eco*RI, *Hin*dIII, and *Xba*I sites (R, X, and H, respectively). Panel B: Detailed map of the 2.2 kb region around the DHFR bidirectional promoter. Black boxes indicate exons. Arrows designate the major and minor DHFR transcription start sites at −63 and −107, as well as the start site for the divergent gene at −195. Two different probes (103CAT and 1.3R1) are shown below the map. In panels A and B, the A in the ATG codon is arbitrarily set at +1. Panel C: Map of a 15 kb region near the 5th intron and 6th exon. Positions of the 1.4 kb probe EX, resected from a cDNA clone (Carothers et al., 1983), and the 1.2 kb INT probe from the 5th intron of the DHFR gene are shown.

The Pattern of Histone−DNA Cross-Links Varies in Different Parts of the DHFR Gene. In order to investigate histone−DNA interactions along the DHFR gene, DMS-

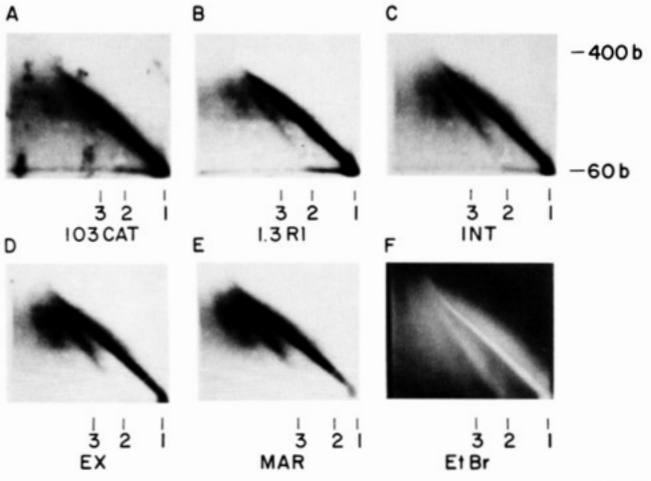

FIGURE 3: Two-dimensional gel analysis of histones cross-linked to DNA by the dimethyl sulfate method. Cross-linking was performed as described in Materials and Methods. Histone−DNA complexes were electrophoretically separated in the first dimension of the gel and were then digested in the gel with proteinase K prior to separation in the second dimension (see Materials and Methods). After transfer to a membrane, the DNA was hybridized with the indicated probes. Probes were removed from transfers as described (Dijkwel & Hamlin, 1988). Diagonal 1 corresponds to free DNA, and diagonals 2 and 3 correspond to DNA cross-linked to the core histones or to histone H1, respectively. Film exposures in panels C, D, and E were chosen so that the intensities of the free DNA diagonals were approximately the same. In panels A and B, exposures were chosen to give twice that intensity in order to detect diagonals 2 and 3, which were faint. Panel F: Ethidium bromide-stained pattern of total genomic histone−DNA cross-linking. (Note that the spots to the left in panel A are a hybridization artifact and do not interfere with the quantitation of signal strengths in the diagonals.)

induced cross-linking experiments were performed after formaldehyde fixation, using a protein imaging method described previously (Karpov et al., 1984; Mirzabekov et al., 1989). DMS transfers a methyl group to the N7 of guanosine or the N3 of adenine, which induces depurination at elevated temperatures. A reactive aldehyde is formed on the C1 of deoxyribose, which can then cross-link to α-amino groups, the ϵ-amino groups of lysines, or the imidazole groups of histidines on nearby proteins. Cross-linking to protein leads to a single-stranded DNA scission resulting from elimination of the 3′ phosphate. Protein−DNA interactions were stabilized by reduction with sodium borohydride (Levina et al., 1981). It has been shown that, under these conditions, histones cross-link to DNA predominantly through histidines (Nacheva et al., 1989).

To identify and quantitate the resulting cross-linked histones in a region of interest, purified DNA−histone complexes are fractionated by a 2-D diagonal gel electrophoretic technique (Mirzabekov et al., 1989). In the first dimension, protein−DNA complexes are separated according to their aggregate molecular weight. The lane containing the resulting spectrum of complexes is excised from the gel, subjected to proteolysis, and run in the second dimension. By this method, the resulting DNA fragments are distributed along three different diagonals, as shown for bulk chromatin in the ethidium bromide-stained pattern in Figure 3F. Diagonal 1 contains un-cross-linked DNA, and diagonals 2 and 3 contain DNA that had been cross-linked to the nucleosomal core histones or to histone H1, respectively (Karpov et al., 1984). The quantity of histones cross-linked in a region of interest can be evaluated by transferring the DNA to a membrane, hybridizing with an appropriate probe, and measuring the integrated volume of each diagonal on autoradiograms by densitometric scanning.

Table 1: Variation of Histone−DNA Cross-Linking in Different Parts of the DHFR Domain

	%				
probe	103CAT	1.2R1	INT	EX	MAR
core histones[a]	<10	22	75	74	100
histone H1[a]	*b*	20	52	65	100

[a] Amount of cross-linked histones was calculated after scanning autoradiograms three times and averaging the three values. The data are expressed as percentages relative to the MAR (see Materials and Methods). [b] Not detectable.

Figure 3A−E shows the results obtained when different regions of the DHFR gene were analyzed (see maps in Figure 2 for probe positions). The 2-D pattern in panel A, which was obtained with an 87 bp probe that straddles the transcription start site (103CAT), is almost devoid of diagonals 2 and 3 even in this somewhat overexposed autoradiogram. Thus, this region of the promoter appears either to be devoid of histones or to interact with histones in a way that lowers their ability to be cross-linked to DNA. A 1.3 kb probe that covers the region extending from −896 to +395 (1.3R1) detects only faint diagonals 2 and 3 (panel B), suggesting that this entire region of the promoter is somewhat depleted of (or interacts differently with) nucleosomes.

In the autoradiograms shown in panels C and D, which were produced with probes from the central part of the 5th intron and the 6th exon, respectively, prominent diagonals 2 and 3 are observed. Thus, these regions of the gene appear to be similar to bulk chromatin, as indicated by their similarity to the ethidium bromide staining pattern (panel F).

The greatest yield of histone−DNA cross-linking was observed in the region of the genome detected by a probe from the downstream matrix-attachment region (MAR; Dijkwel & Hamlin, 1988; Figure 3E). As we will show below, this region also displays the lowest efficiency of DNA methylation, the longest nucleosomal repeat, and the most distinct nucleosomal ladder among all of the regions analyzed in this study. Thus, the very regular chromatin organization in the MAR region serves as an internal standard against which to compare other regions of the DHFR gene.

As shown in Table 1, the amounts of diagonals 2 and 3 are at least 5-fold lower in the region detected with probe 1.3R1 (−896 to +395) than with the MAR probe. The amounts of diagonals 2 and 3 detected with the 103CAT probe, which lies directly over the promoter, are less than 10% of the MAR signal and too weak to be detected over background. The quantities of cross-linked core histones in the central part of the 5th intron and in the 6th exon are ~25% lower than in the MAR region, and both regions (particularly the intron) show decreased levels of H1 histone relative to the MAR.

The Chromatin in the 5′ Flanking Region of the DHFR Gene Is More Sensitive to DNA Methylation Than in the 3′

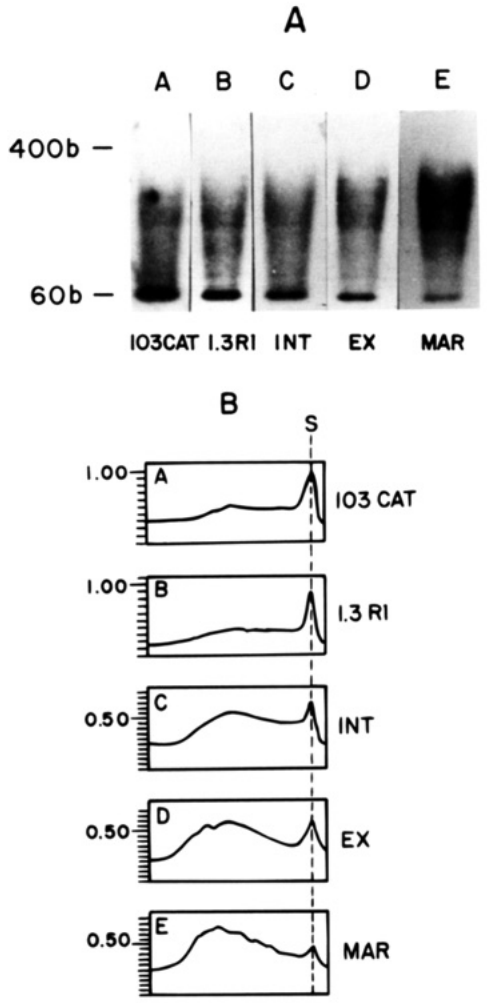

FIGURE 4: Efficiency of methylation of the DHFR gene with DMS. Nuclei were fixed with formaldehyde and methylated with DMS, and the methylated DNA sites were cleaved as described in Materials and Methods. The DNA was purified, separated on a polyacrylamide gel in 7 M urea, and transferred by electroblotting to GeneScreen Plus. The blot was hybridized sequentially with probes and exposed to film. Panel A: Hybridization probes were as follows: lanes A and B, the promoter region (probes 1.3R1 and 103CAT in Figure 2B, respectively); lane C, the 5th intron (INT in Figure 2); lane D, the 6th exon (probe EX, Figure 2); lane E, the MAR probe. Sizes of single-stranded markers are indicated on the left. Panel B: Scans of the autoradiograms shown in panel A. "S" denotes the position of the compression zone of unseparated DNA fragments (<~60 bp). Note that the scales of optical density differ by a factor of 2 between the upper and lower panels.

Region. We next determined the relative accessibility of various segments of the gene to methylation by DMS. Nuclei were first subjected to formaldehyde fixation and were incubated with DMS, as in the protein−DNA cross-linking experiments. However, in this approach, samples were then boiled in a solution containing a primary amine (Tris-HCl) to induce excision of methylated purines and single-strand scissions at apurinic sites (Levina et al., 1981) (Figure 1, method 2).

The relative efficiencies of DNA methylation by DMS in different parts of the DHFR gene were determined by comparing the average lengths of the excised fragments from each region: the higher the efficiency of methylation, the lower the average length of the fragments is expected to be. In the denaturing 6% polyacrylamide gels shown in Figure 4A, fragments greater than ~60 bp in length migrate to their appropriate positions in the gel, whereas fragments less than ~60 bp do not resolve from one another and stack in a relatively tight and easily quantifiable band. After electrotransfer of DNA fragments to a membrane, the blots were hybridized with different probes and the resulting autoradiographic images were scanned in a densitometer to give a semi-quantitative picture of methylation site distributions (the stack is labeled "S" in Figure 4B).

In the scans corresponding to the 5′ region of the gene (probes 103CAT and 1.3R1 in panels A and B, respectively), the higher molecular weight peak is greatly diminished relative to the standard MAR region (panel E), and the S peak is ~3-fold higher. With the MAR probe (panel E), the high molecular weight peak is centered at ~300 nt and its height is roughly twice that of the S peak. In the scans of DNA fragments from the 5th intron and 6th exon, the high molecular weight peak shifts to ~250 nt and the region greater than 300 nt is somewhat diminished relative to the MAR. The greatest amount of larger fragments and the least amount of small fragments (peak S) are observed in the MAR region (panel E).

These data indicate that the chromatin in the 5′ end of the gene is the most accessible to DMS. Since the average length of DNA fragments decreases as the rate of DNA methylation by DMS increases, the efficiency of methylation (accessibility) of the different chromatin regions analyzed in this experiment is as follows: 103CAT > 1.3R1 > 5th intron > 6th exon > MAR.

Nucleosome Organization Is Disturbed in the 5′ Region of the Gene. The distribution of nucleosomes in the DHFR gene was assessed by subjecting isolated nuclei to partial digestion with micrococcal nuclease, separating the DNA fragments on a 1.5% agarose gel, and hybridizing a transfer of the digests with selected probes (Figure 1, method 3).

Hybridization with the 1.3R1 probe (Figure 5, lane B) reveals a complex pattern. The sizes of most fragments do not correspond to multimers of the usual nucleosomal repeat length (180−200 bp), and the intensities and widths do not change monotonically, as is the case with the MAR region (Figure 5, lane E). More than 20 prominent fragments are superimposed on the underlying smear of bands and are arranged in an irregular manner. In most cases, the difference in the length between two neighboring bands is less than 145 bp (the size of the region protected by one nucleosomal core). The most prominent bands are 435, 545, 970, 1475, 2985, and 3400 bp in length. Discrete bands can still be resolved at the top of the gel (e.g., fragments at 5.9 and 6.2 kb). [Note that data could not be obtained for the 103CAT probe owing to its small size (87 bp) and the consequent difficulty in obtaining a probe with a high enough specific radioactivity.]

In contrast, probes from the 5th intron, the 6th exon, and the MAR (Figure 5, lanes C−E) all display the regular repeating pattern characteristic of the canonical nucleosome organization observed in bulk chromatin. The nucleosomal repeat lengths are 180, 188, 194, and 181 bp in the 5th intron, 6th exon, MAR, and bulk chromatin, respectively. The autoradiographic exposures in these experiments were adjusted so that the nucleosomal ladders were approximately the same intensity for different probes. Under these circumstances, we found that the overall pattern of the nucleosomal ladder in the 5th intron is somewhat more diffuse, is superimposed against a higher background, and

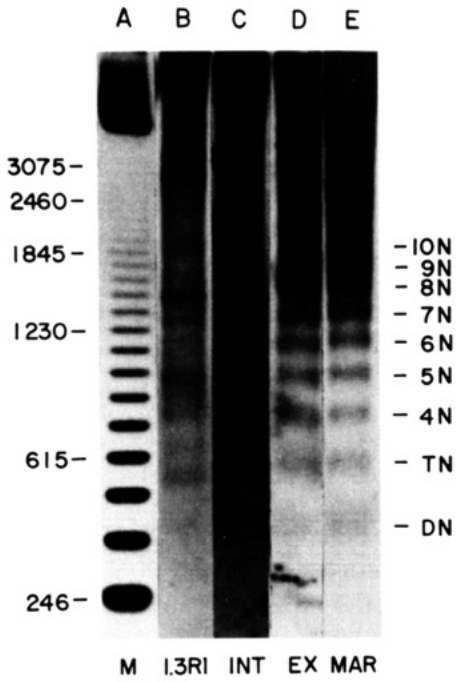

FIGURE 5: Micrococcal nuclease digestion of chromatin in different parts of the DHFR domain. Isolated nuclei were treated with micrococcal nuclease, and the DNA was purified as described in Materials and Methods. The resulting DNA fragments were separated on a 1.5% agarose gel. Lane A contains a ^{32}P-labeled 123 bp ladder for size markers. Lanes B−E contain DNA fragments from the micrococcal digest hybridized with the indicated radioactive probes (see Figures 2 and 7 for probe positions). Di-, tri-, tetranucleosomes, etc., are denoted by numbers to the right.

displays a reduced nucleosomal repeat length. The region also displays a decreased number of nucleosomal bands relative to the MAR. Only 7 or 8 nucleosomes can be discerned in the INT ladder, while the bands corresponding to 10 and 11 nucleosomes are well discriminated in the MAR ladder.

The Pattern of Micrococcal Nuclease Cutting Sites in the 5′ Region of the DHFR Gene Is Grossly Altered Relative to Naked DNA. To obtain a detailed picture of the locations of proteins and positioned nucleosomes within various regions of the DHFR gene, the patterns of micrococcal nuclease cutting sites in chromatin were compared to those in naked DNA. Digestion was performed so as to yield only one cut per ~10 000 kb of DNA. After purification, the DNA was further digested to completion with either *Xba*I or *Hin*dIII to allow any hypersensitive sites to be mapped relative to fixed restriction sites. The digests were separated on a 1.5% agarose gel, transferred to a membrane, and analyzed by indirect end-labeling (Nedospasov & Georgiev, 1980; Wu, 1980).

To detect micrococcal nuclease cutting sites lying within the 5′ region of the gene, the 1.3R1 probe was utilized as a label for either the 7.2 kb *Xba*I (covering the region from −6240 to +940 bp) or the 7.25 kb *Hin*dIII fragment (covering −1240 to +6010). These fragments overlap one another in the area of the promoter (from −1240 bp to +940 bp; Figures 6E and 8), which can therefore be mapped with enhanced accuracy (for example, nine cut sites, including four hypersensitive sites, could be mapped between −635 and +150 bp with a resolution of ±5 bp; see below).

The results obtained with the 1.3R1 probe are shown in Figure 6A,B (*Xba*I digest; two different film exposures are presented to illuminate details in different parts of the gel) and in Figure 6C,D (*Hin*dIII). The pattern of micrococcal nuclease cutting sites in chromatin differs markedly from the pattern in the corresponding naked DNA sample. In fact, of the 53 chromatin sites that can be resolved in the two exposures, none (with the exception of band 40) appears to behave identically to the corresponding sequence in naked DNA: either a site disappears, a new site appears, or a band is weakened or enhanced in chromatin.

A summary of the data in the promoter region is shown in Figure 6E. In this map, numbered arrows indicate novel cutting sites (i.e., not observed in DNA), while numbered open circles and boxes indicate diminished or enhanced cutting, respectively, of sites also detectable in naked DNA. The many alterations in chromatin in this region can be used to create a picture of protein interactions, as we will do in the Discussion.

To obtain information about chromatin architecture in the 5th intron and the 6th exon, the *Xba*I blot was rehybridized (after removing the previous probe) with the INT or the EX probes (see maps, Figure 2A,C, and Figure 7). (Note that the DNA and chromatin lanes are reversed relative to Figure 6.) The patterns of hydrolysis of chromatin and free DNA in the 3′ region of the gene (represented by the 5.0 and 4.5 kb *Xba*I fragments; see map, Figure 2C) are very similar (Figure 7A,B), except for the 2.3 kb region near the center of the 5th intron (Figure 7C), mapping between +16.6 and +18.9 kb (Figure 2A). Three bands (1, 4, and 9) disappear in chromatin, and one new band (5) appears. The intensity of bands 2 and 8 increases in chromatin, while that of 3, 6, 7, and 10 decreases. Note that the intensified bands 2, 3 and 5, and 8 and 10 are clustered around the bands that are lost (1, 4, and 9). Changes of this type are typical in regions of specific protein interactions or positioned nucleosomes (Elgin, 1988; Gross & Garrard, 1988; Simpson, 1991).

DISCUSSION

Histone−DNA Cross-Linking. It is important to point out that in the histone−DNA cross-linking and DNA methylation experiments, the size of the genomic region characterized by blot hybridization may be considerably larger than the hybridization probe itself. For example, the 103CAT probe can detect sequences extending ~200 bp upstream and downstream from the 87 bp fragment itself; this follows, since the longest DNA fragments in the gels shown in Figures 3A and 4A (panel A) are about 300 bp, and the efficiency of probe hybridization is markedly decreased when overlap with the target fragment is less than ~100 bp. However, with probes 1.3R1, INT and EX, which are 1.3, 1.2, and 1.4 kb in length, respectively (Figure 2), the length of DNA detected coincides approximately with the probe sizes themselves.

The histone−DNA cross-linking study demonstrates that the histone content can vary considerably in different parts of the gene, in agreement with earlier work on other genes (Belikov et al., 1990, 1993; Nacheva et al., 1989). The yield of cross-linked histones is dramatically reduced in the 1.3 kb region from −900 to +400 (Figure 3B) and especially in the promoter region between −300 and +200 (Figure 3A). In the 3′ end of the gene (the 5th intron and the 6th exon), the yield of core histones cross-linked to DNA is reduced by ~25% relative to the MAR (Table 1). Surprisingly, the

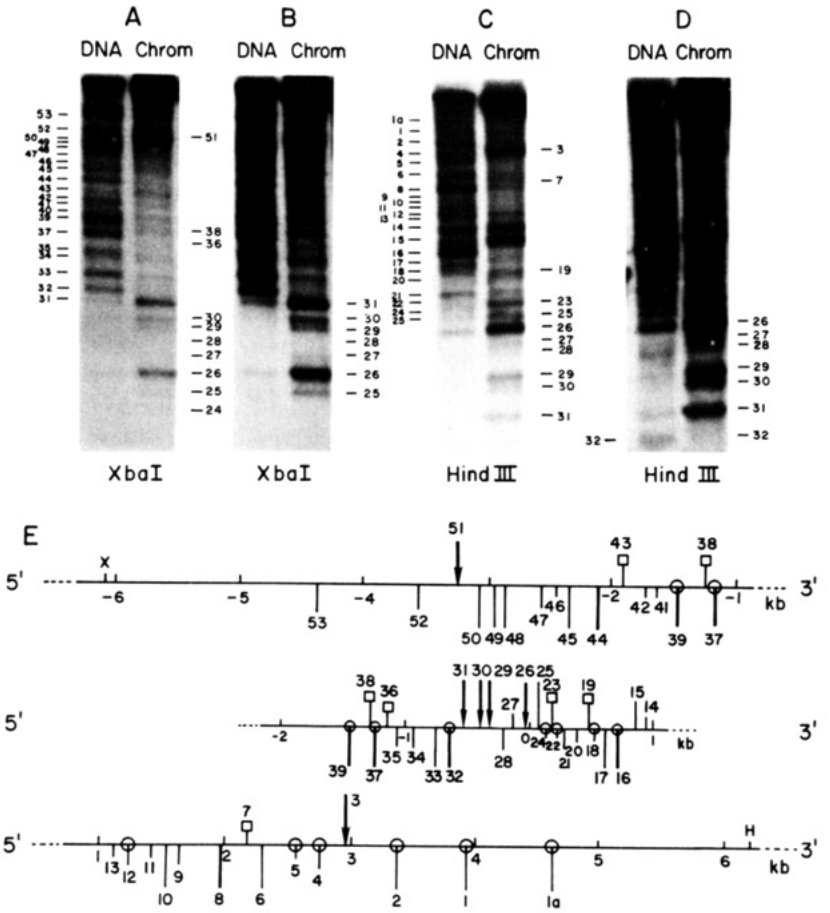

FIGURE 6: Positions of micrococcal nuclease-hypersensitive sites in the promoter region of the DHFR gene. Panels A–D: DNA and isolated nuclei were digested with micrococcal nuclease and, after RNAase treatment, were deproteinized and digested to completion with *Xba*I (panels A and B) or *Hin*dIII (panels C and D). Two different autoradiographic exposures are shown for each digest. After separation on a 1.5% agarose gel and transfer to GeneScreen Plus, the digests were hybridized with probe 1.3R1. Panel E: A detailed map of the 12 kb region surrounding the DHFR promoter, showing the positions of hypersensitive cutting sites in chromatin (arrows), new sites (boxes), masked sites (open circles), or enhanced or diminished cutting sites (upward- or downward-directed lines) relative to naked DNA. The length and width of the latter two lines corresponds approximately to the degree of enhancement or diminution. All 53 sites that could be resolved on these gels are shown. The A of the ATG codon for the DHFR gene is set at +1.

efficiency of histone H1 cross-linking to DNA is especially reduced in a 1.2 kb region in the central part of the 5th intron (from +18.35 kb to +19.55 kb; Figure 3C).

These data suggest either the loss of histones or a considerable alteration of histone–DNA interactions in the nucleosomes in these two regions. In these experiments, histones were cross-linked to DNA predominantly through histidine residues (Nacheva et al., 1989). Most histidines are found in the globular parts of histones (Wu et al., 1986), and it has been shown previously that, in the coding region of the actively transcribed hsp70 gene of *Drosophila melanogaster*, histones lose most of their histidine–DNA contacts but interact with DNA predominantly through their lysine-rich tails (Nacheva et al., 1989). These changes probably reflect the disruption of most of the nucleosomes in the hsp70 gene because of the high level of transcriptional activity and the attendant high density of RNA polymerases, as with ribosomal genes (Labhart & Koller, 1982).

The DHFR gene, on the other hand, is a housekeeping gene whose transcriptional activity is probably considerably lower than that of hsp70 and ribosomal genes. This is suggested by the fact that the yield of histone–DNA cross-linking in a coding part of the gene (i.e., the 6th exon) is only slightly different than the chromatin of the MAR control sequence (Figure 3F,E). This result was obtained in spite of the fact that the DHFR gene is transcribed mainly in the late G_1 and early S periods, and the CHOC 400 cells analyzed in these experiments were not synchronized. Thus, we conclude that the loss of (or altered interaction with) nucleosomes in the 5′ region of the gene probably exists throughout most of the cell cycle.

Although the 103CAT probe detects virtually no histone–DNA cross-links (Figure 3A), the larger 1.3R1 probe detects ~22% as many cross-links as the MAR probe (Figure 3B,E). This suggests either that part of the 1.3 kb R1 fragment is structured like bulk chromatin or that there are occasional single nucleosomes distributed throughout this fragment (excluding the 100 bp 103CAT region itself). Alternatively, the histones in this region may conserve 22% of their interactions via the globular parts of histones inherent in bulk chromatin. Or perhaps 22% of the genes are actually inactive and therefore display the interaction with nucleosomes that characterizes bulk chromatin.

It should also be emphasized that isolated nuclei were reversibly fixed in formaldehyde prior to DMS cross-linking. Hence, the failure to detect significant quantities of cross-linked histones in the 5′ region of the gene is probably not a consequence of histone removal during the cross-linking procedure, which, indeed, can take place in regions of active

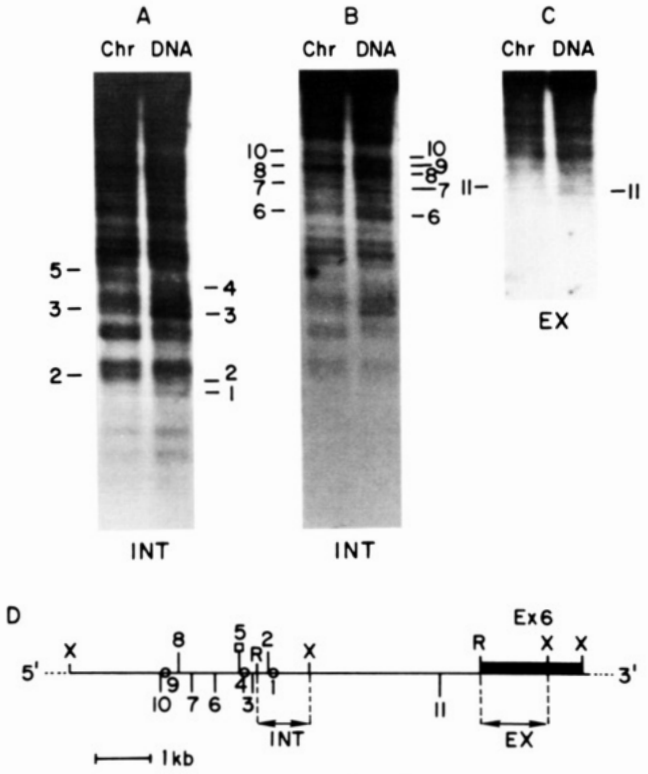

FIGURE 7: Positions of micrococcal nuclease hypersensitive sites in the 3′ region of the DHFR gene. Panels A and B: Same blot of the *Xba*I digest shown in Figure 6A,B, except probed with the 3′ INT probe. Two different exposures are shown. Panel C: Same as panel A, except probed with the 3′ EX probe. Panel D: Map showing relevant restriction sites and positions of the INT and EX probes. For notations, see Figure 6.

chromatin in the absence of formaldehyde fixation (Bavykin et al., 1993).

DNA Methylation with DMS. Along with enzymatic and chemical nucleases, DMS has been profitably employed to study protein−DNA interactions, using either indirect end-labeling or footprinting methods to identify affected DNA residues (Elgin, 1988; Gross & Garrard, 1988; McGhee & Felsenfeld, 1979; Mueller & Wold, 1989; Sigman, 1990; Thoma, 1988; Tullius et al., 1987). It has been shown previously that histones in isolated nucleosomal particles do not protect DNA from methylation by DMS (McGhee & Felsenfeld, 1979). However, it has also been shown that, *in vivo*, histones can partially shield the DNA from methylation by DMS (Mirzabekov et al., 1977). In the present study, we have used DMS for the first time to estimate the level of sensitivity of different regions of a gene to chemical methylation.

We have shown that the efficiency of DNA methylation in formaldehyde-fixed nuclei is inversely proportional to the amount of histones detected by DMS-induced cross-linking in every region of the DHFR gene examined. We suggest that the absence of detectable histone cross-linking in a particular region may be due either to the absence of histones or to the presence of nucleosomes that constrain the DNA without requiring the participation of histidines.

The rate of methylation increases in the order MAR < EX < INT < 1.3R1 < 103CAT, while the amount of cross-linked histones decreases in the order MAR > EX > INT > 1.3R1 > 103CAT (Figures 3 and 4 and Table 1). The same result was obtained by hybridizing the same blot with a number of probes from different parts of the DHFR domain, including the downstream replication initiation locus (unpublished observations).

Micrococcal Nuclease Digestion of Chromatin in Isolated Nuclei. The relationship between the nucleosomal repeat value and transcriptional activity in chromatin has been addressed repeatedly. It has been shown with some genes that the distance between two neighboring core particles is lower in transcriptionally active genes than it is in silent regions (e.g., Cartwright et al., 1982; Igo-Kemenes et al., 1982), but contradictory results have been obtained (Reeves, 1984; Yaniv & Cereghini, 1986).

In the present study, the results of histone−DNA cross-linking and DNA methylation efficiency in different parts of the DHFR gene are in good agreement with the pattern and extent of hydrolysis by micrococcal nuclease. In the 5′ region of the gene, where the amount of histones/DNA cross-links is greatly reduced and the rate of methylation is increased, the regular nucleosomal organization of chromatin is interrupted for at least 1.2 kb (i.e., from −900 to +400, the position of the 1.3R1 probe; Figures 5B and 2B).

In addition, when a digest showing a clear nucleosomal ladder for bulk chromatin (assessed from ethidium bromide staining) was hybridized with the 1.3R1 probe, a number of discrete (but irregular) bands was observed, some of them as long as 6.2 kb (Figure 5B). These data indicate that the regular nucleosomal ladder is disrupted in a region at least 6.2 kb in length. It is likely that this region is bounded by the two hypersensitive sites at −3260 and +2960 (Figure 6E).

In the strictest sense, however, the absence of a canonical nucleosomal ladder cannot be taken as proof that nucleosomes are absent from a chromosomal region. As has been shown previously, nucleosomes in the upstream regions of some constitutively expressed genes can be arranged as oligonucleosomal islands separated from one another by spacer DNA of various lengths (Tazi & Bird, 1990). Alternatively, disturbance of the nucleosomal ladder may indicate that the chromatin in a region is arranged as positioned nucleosomes and/or contains nucleosome-free DNA zones that are organized in complexes with trans-acting factors (Elgin, 1988; Gross & Garrard, 1988; Simpson, 1991).

Hybridization of the micrococcal nuclease partial digest with a probe from the central part of the last intron (in which the level of histone−DNA cross-linking and the rate of methylation are intermediate between those of the 5′ region and the MAR) reveals a prominent nucleosomal ladder (Figure 5C). However, the ladder is superimposed on a relatively high and uniform background, which has been observed for other actively transcribed genes (Kornberg & Lorch, 1992); in addition, a reduced number of nucleosomal bands relative to the 6th exon and the MAR could be resolved in the ladder, and the nucleosomal repeat length was decreased (180 bp as opposed to 194 bp for the region detected with the MAR probe).

The pattern of chromatin hydrolysis with micrococcal nuclease probably reflects several aspects of chromatin architecture, including higher order structure, the relative amount of histones in a particular region, and the way in which the histones interact with DNA. Recently we have shown that the composition of the mononucleosomal set excised with micrococcal nuclease depends on chromatin higher order structure (Bavykin et al., 1990). Again,

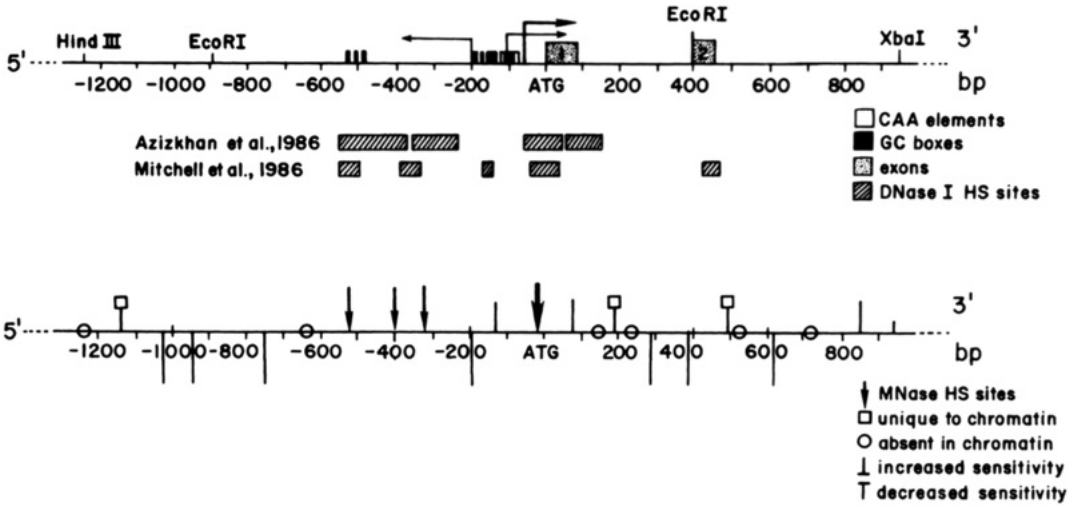

FIGURE 8: Summary of data and model for chromatin organization in the promoter of the DHFR gene. The upper panel shows a functional map of the DHFR gene, with the A in the ATG codon corresponding to position +1. The open and black boxes above the scale indicate the CAA and GC box elements, respectively. The stippled boxes indicate the position of DHFR exons, and the arrows indicate the major and minor DHFR transcription start sites at −63 and −107, as well as the start site for the divergent transcript at −195. A summary of DNaseI-hypersensitive sites detected in previous studies (Azizkhan et al., 1986; Mitchell et al., 1986). Lower panel: Same map and scale, indicating positions of micrococcal nuclease cutting sites. Arrows indicate micrococcal nuclease hypersensitive sites, boxes indicate new bands in chromatin that are not detected in naked DNA, and circles indicate inaccessible regions that are detected in naked DNA. The vertical lines above and below the scale indicate bands that either increase or decrease in chromatin relative to corresponding sites in DNA.

weakening of the interaction of the globular part of histones in the core particle upon chromatin unfolding (S. I. Usachenko, I. M. Gavin, and S. G. Bavykin, unpublished observations), changes of nucleosome positioning in unfolded chromatin (Thoma & Zatchej, 1988), or loss of nucleosomes from functionally active regions of the genome may result in changes of nucleosomal structure in such a region (Evans et al., 1990; Kornberg & Lorch, 1992). This may lead to an attenuated nucleosomal ladder (high background, reduced number of nucleosomal bands) and a decreased nucleosomal repeat length probably due to rearrangements of nucleosomes during hydrolysis with micrococcal nuclease (Smith et al., 1984; Widmer et al., 1987).

The nucleosomal organization of the 6th exon proves to be closest to the MAR (Figure 5D,E), and this is the region in which the amount of histones cross-linked to DNA is the highest and the rate of methylation is the lowest among the parts of the gene examined in this study.

Our results indicate that the nucleosomal repeat may be different in neighboring parts of the same gene (this further suggests that the value of the nucleosomal repeat depends on factors in addition to the transcriptional state of the gene) and varies widely throughout the DHFR domain (from 180 bp in the 5th intron to 194 bp in the MAR). Our estimate for nucleosomal repeat length in the bulk chromatin of CHOC 400 cells (181 bp) does not differ significantly from the 178 bp value estimated for CHO cells by Compton et al. (1976) and by us (unpublished observations). However, Rill and co-workers estimate the repeat length in CHO cells to be 172−173 bp (Rill et al., 1977). The reason for this discrepancy is presently not clear.

Mapping Preferred Micrococcal Nuclease Cut Sites in the Chromatin of the DHFR Gene. The indirect end-labeling method is commonly used to analyze regions of the genome with functional significance (e.g., promoters) for any unusual (non-nucleosomal) chromatin arrangements. The use of DNaseI has allowed detection of extended nucleosome-free regions up to 1.3 kb in length (e.g., Bellard et al., 1986). The spectrum of hypersensitive sites revealed by micrococcal nuclease and DNaseI are very similar (Gross & Garrard, 1988; Simpson, 1991). However, micrococcal nuclease offers a much more detailed picture, revealing precisely positioned nucleosomes and the locations of trans-acting factors (Gross & Garrard, 1988; Thoma, 1988).

Our indirect end-labeling experiments with micrococcal nuclease revealed a number of hypersensitive sites in the 5′ region of the gene, but not in the 3′ region (Figures 6 and 7). The hypersensitive sites detected in the promoter of the DHFR gene in CHOC 400 cells (Figure 8) coincide approximately with those deduced earlier using DNaseI on isolated nuclei from CHO UK3 cells (Mitchell et al., 1986) and from CHOC 400 cells (Azizkhan et al., 1986); these two methotrexate-resistant cell lines contain 300 and 1000 copies of the DHFR gene, respectively. These findings may indicate that, as with the human DHFR gene (Shimada et al., 1987), chromatin structure is dictated by the underlying DNA sequence.

Indirect end-labeling experiments show that hypersensitive sites are organized in two separate clusters in the bidirectional promoter: between −150 and +100 and between −300 and −550 (Figure 8). The strongest hypersensitive site is located in the region proximal to the ATG codon at −20 bp, with a neighboring site of increased sensitivity at −133 bp (Figure 8); this region contains the major and minor transcription start sites of the DHFR gene at −63 and −107, respectively (Mitchell et al., 1986). Another site displaying increased sensitivity maps at +80 bp in the proximal region (Figure 8). In contrast, a site with decreased sensitivity to micrococcal nuclease digestion was located at −200 bp (Figure 8) in the neighborhood of the transcription start site for the divergent gene at −195 bp (Mitchell et al., 1986). Three other somewhat weaker hypersensitive sites were detected upstream at −325, −403, and −522. Interestingly, the DNA sequence in this latter region is ~70% identical to a sequence in the human gene to which a multiprotein complex was mapped (Mitchell et al., 1986; Shimada et al., 1986). Two

additional strong hypersensitive sites were found at about −3260 and +2960 (Figure 6E). The indirect end-labeling studies on micrococcal nuclease digests also revealed that chromatin architecture is dramatically rearranged in a region 9 kb in length extending from −4300 bp (site 53) to +4700 bp (site 1a) (Figure 6E). The sensitivities of more than 50 cut sites were found to be altered in chromatin relative to naked DNA (Figure 6A−D).

With the exception of the 2.3 kb region in the central part of the 5th intron, we did not find significant differences in micrococcal nuclease patterns between DNA and chromatin in the 3′ region of the gene (Figure 7). Together with histone−DNA cross-linking data (Figure 3C,D), these data argue that nucleosomes are distributed randomly along the DNA in most of the 3′ region of the gene.

Chromatin Architecture in the 5′ and 3′ Regions of the DHFR Gene. In total, data from the four different experimental approaches used in this study show that the chromatin structure in the 5′ and 3′ regions of the Chinese hamster DHFR gene differs markedly from bulk chromatin.

Two zones of hypersensitivity were detected in the 5′ region, one near the ATG codon (−150 to +100) and one lying further upstream (−550 to −300). We found that the interactions with histones through their globular domains, which characterize condensed chromatin (Kornberg & Lorch, 1992), are dramatically decreased in the region from −900 to +400 compared to the MAR region, especially around the promoter from −300 to +200 (Figure 3A,B). We suggest that both distal and proximal hypersensitive zones are devoid of nucleosomes, because the distance between the hypersensitive sites in this region are too short to accommodate a nucleosome (Figure 8). In addition, the positions of these zones coincide remarkably well with previously detected zones of hypersensitivity to DNaseI, which are believed to be nucleosome-free (Azizkhan et al., 1986; Mitchell et al., 1986; for a review, see Gross & Garrard, 1988).

In the regions upstream from the distal hypersensitive zone (−550 to −900), downstream from the proximal zone (+100 to +400), and between them (−300 to −150), a nucleosome could theoretically exist. However, these regions either do not organize nucleosomes, or any resident nucleosomes have an altered structure relative to nucleosomes in bulk chromatin or the MAR region, because of the marked attenuation of histidine contacts in the globular regions of histones with DNA (Figure 3A,B and Table 1).

Moreover, an examination of partial micrococcal nuclease digestion products either in nucleosomal ladders or by indirect end-labeling (Figures 5B and 6) shows that the entire region lying between −4.3 and +4.7 kb is organized in a configuration distinct from bulk chromatin. Much of this region is likely to contain nucleosomes positioned over specific DNA sequences and/or nucleosome-free zones that interact with a number of trans-acting factors.

By contrast, no hypersensitive sites were detected in the 3′ end of the DHFR gene and, with the exception of the central part of the 5th intron, nucleosomes appear to be arranged randomly. However, the chromatin in the central part of the 5th intron displays some features characteristic of active chromatin (Kornberg & Lorch, 1992), i.e., decreased efficiency of interaction between the globular parts of histone and DNA (Figure 3D and Table 1) and loss of definition (smearing) of the nucleosomal ladder (Figure 5C). Moreover, a 2-fold reduction in histone H1−DNA cross-linking relative to the MAR (Table 1), the increased sensitivity of DNA to methylation with DMS relative to the MAR (Figure 4A, panel D), the decreased nucleosomal repeat length (Figure 5C), and specific changes in sensitivity to micrococcal nuclease digestion revealed by indirect end-labeling (Figure 7) all suggest that this region may play some functional role. In particular, the juxtaposition of sites with both increased and decreased sensitivity to micrococcal nuclease digestion in this intronic region (Figure 7) could indicate the binding of specific proteins rather than the presence of positioned nucleosomes, since such proteins often distort the conformation of DNA and render it more accessible to nuclease digestion (Travers, 1989).

Since no prior information suggested the presence of any functional elements in the fifth intron of this gene, it has not yet been sequenced. Therefore, at present, we cannot speculate as to the significance, if any, of altered chromatin structure in this region of the gene.

The chromatin architecture of the DHFR gene has also been investigated in human cells containing ~80 copies of the DHFR domain (Shimada et al., 1986). The essential similarity in the distribution of conservative sequence elements in the 5′ region of the gene in hamsters and humans is reflected in the chromatin structure. As was shown (Shimada et al., 1986), there is a nucleosome-free region from −830 bp to +80 bp relative to the ATG codon. This region is subdivided into two DNaseI-hypersensitive sections that include proximal and distal clusters of GC boxes and which are separated by a relatively DNaseI-resistant section lying between −410 and −240 bp. This resistant section is believed to be occupied by a multiprotein complex (Shimada et al., 1986). Further upstream and downstream from −830 and +80 bp, respectively, the nucleosomal repeating structure is re-established.

ACKNOWLEDGMENT

We would like to thank Jane Azizkhan (Roswell Park) for the gift of plasmid 103CAT and the members of our laboratory for useful discussions.

REFERENCES

Azizkhan, J. C., Vaughn, J. P., Christy, R. J., & Hamlin, J. L. (1986) Nucleotide sequence and nuclease hypersensitivity of the Chinese hamster dihydrofolate reductase gene promoter region. *Biochemistry 25*, 6228−6236.

Bavykin, S. G., Usachenko, S. I., Zalensky, A. O., & Mirzabekov, A. D. (1990) Structure of nucleosomes and organization of internucleosomal DNA in chromatin. *J. Mol. Biol. 212*, 495−511.

Bavykin, S., Srebreva, L., Banchev, T., Tsanev, R., Zlatanova, J., & Mirzabekov, A. (1993) Histone H1 deposition and histone−DNA interactions in replicating chromatin. *Proc. Natl. Acad. Sci. U.S.A. 90*, 3918−3922.

Belikov, S. V., Dzherbashyajan, A. R., Preobrazhenskaya, O. V., Karpov, V. L., & Mirzabekov, A. D. (1990) Chromatin structure of Drosophila melanogaster ribosomal genes. *FEBS Lett. 273*, 205−207.

Belikov, S. V., Belgovsky, A. I., Preobrazhenskaya, O. V., Karpov, V. L., & Mirzabekov, A. D. (1993) Two non-histone proteins are associated with the promoter region and histone H1 with the transcribed region of active hsp-70 genes as revealed by UV-induced DNA−protein crosslinking in vivo. *Nucleic Acids Res. 21*, 1031−1034.

Bellard, M., Dretzen, G., Bellard, F., Kaye, J. S., Pratt-Kaye, S., & Chambon, P. (1986) Hormonally induced alterations of

chromatin structure in the polyadenylation and transcription termination regions of the chicken ovalbumin gene. *EMBO J. 5*, 567−574.

Blake, M. C., Jambou, R. C., Swick, A. G., Kahn, J. W., & Azizkhan, J. C. (1990) Transcriptional initiation is controlled by upstream GC box interactions in a TATA-less promoter. *Mol. Cell. Biol. 10*, 6632−6641.

Buermeyer, A. B., Thompson, N. E., Strasheim, L. A., Burgess, R. R., & Farnham, P. J. (1992) The HIP1 initiator element plays a role in determining the in vitro requirement of the dihydrofolate reductase gene promoter for the C-terminal domain of RNA polymerase II. *Mol. Cell. Biol. 12*, 2250−2259.

Carothers, A. M., Urlaub, G., Ellis, N., & Chasin, L. A. (1983) Structure of the dihydrofolate reductase gene in Chinese hamster ovary cells. *Nucleic Acids Res. 11*, 1997−2012.

Cartwright, I. L., Abmayr, S. M., Fleischmann, G., Lowenhaupt, K., Elgin, S. C. R., Keene, M. A., & Howard, G. C. (1982) Chromatin structure and gene activity: the role of nonhistone chromosomal proteins. *CRC Crit. Rev. Biochem. 13*, 1−86.

Chen, M. J., Shimada, T., Moulton, A. D., Cline, A., Humphries, R. K., Maizel, J., & Nienhuis, A. W. (1984) The functional human dihydrofolate reductase gene. *J. Biol. Chem. 259*, 3933−3943.

Compton, J. L., Bellard, M., & Chambon, P. (1976) Biochemical evidence of variability in the DNA repeat length in the chromatin of higher eukaryotes. *Proc. Natl. Acad. Sci. U.S.A. 73*, 4382−4386.

Crouse, G. F., Leys, E. J., McEwan, R. N., Frayne, E. G., & Kellems, R. E. (1985) Analysis of the mouse dhfr promoter region: existence of a divergently transcribed gene. *Mol. Cell. Biol. 5*, 1847−1858.

Dijkwel, P. A., & Hamlin, J. L. (1988) Matrix attachment regions are positioned near replication initiation sites, genes, and an interamplicon junction in the amplified dihydrofolate reductase domain of Chinese hamster ovary cells. *Mol. Cell. Biol. 8*, 5398−5409.

Dijkwel, P. A., Vaughn, J. P., & Hamlin, J. L. (1991) Mapping of replication initiation sites in mammalian genomes by two-dimensional gel analysis: stabilization and enrichment of replication intermediates by isolation on the nuclear matrix. *Mol. Cell. Biol. 11*, 3850−3859.

Dynan, W. S., Sazer, S., Tjian, R., & Schimke, R. T. (1986) Transcription factor Sp1 recognizes a DNA sequence in the mouse dihydrofolate reductase promoter. *Nature 319*, 246−248.

Elgin, S. C. R. (1988) The formation and function of DNase I hypersensitive sites in the process of gene activation. *J. Biol. Chem. 263*, 19259−19262.

Evans, T., Felsenfeld, G., & Reitman, M. (1990) Control of globin gene transcription. *Annu. Rev. Cell Biol. 6*, 95−124.

Farnham, P. J., & Schimke, R. T. (1986) Murine dihydrofolate reductase transcripts through the cell cycle. *Mol. Cell. Biol. 6*, 365−371.

Farnham, P. J., & Means, A. L. (1990) Sequences downstream of the transcription initiation site modulate the activity of the murine dihydrofolate reductase promoter. *Mol. Cell. Biol. 10*, 1390−1398.

Fujii, H., E. Shinya, & Shimada, T. (1992) A GC Box in the bidirectional promoter is essential for expression of the human dihydrofolate reductase and mismatch repair protein 1 genes. *FEBS Lett. 314*, 33−36.

Gross, D. S., & Garrard, W. T. (1988) Nuclease hypersensitive sites in chromatin. *Annu. Rev. Biochem. 57*, 159−197.

Hamlin, J. L., & Ma, C. (1990) The mammalian dihydrofolate reductase locus. *Biochim. Biophys. Acta 1087*, 107−125.

Igo-Kemenes, T., Horz, W., & Zachau, H. G. (1982) Chromatin. *Annu. Rev. Biochem. 51*, 89−121.

Karpov, V. L., Preobrazhenskaya, O. V., & Mirzabekov, A. D. (1984) Chromatin structure of hsp 70 genes, activated by heat shock: selective removal of histones from the coding region and their absence from the 5′ region. *Cell 36*, 423−431.

Kornberg, R. D., & Lorch, Y. (1992) Chromatin structure and transcription. *Annu. Rev. Cell Biol. 8*, 563−587.

Labhart, P., & Koller, T. (1982) Structure of the active nucleolar chromatin of Xenopus laevis oocytes. *Cell 28*, 279−292.

Levina, E. S., Bavykin, S. G., Shick, V. V., & Mirzabekov, A. D. (1981) The method of crosslinking histones to DNA partly depurinated at neutral pH. *Anal. Biochem. 110*, 93−101.

Linton, J. P., Yen, J. Y., Selby, E., Chen, Z., Chinsky, J. M., Liu, K., Kellems, R. E., & Crouse, G. F. (1989) Dual bidirectional promoters at the mouse dhfr locus: Cloning and characterization of two mRNA classes of the divergently transcribed Rep-1 gene. *Mol. Cell. Biol. 9*, 3058−3072.

Looney, J. E., & Hamlin, J. L. (1987) Isolation of the amplified dihydrofolate reductase domain from methotrexate-resistant Chinese hamster ovary cells. *Mol. Cell. Biol. 7*, 569−577.

Ma, C., Looney, J. E., Leu, T.-H., & Hamlin, J. L. (1988) Organization and genesis of dihydrofolate reductase amplicons in the genome of a methotrexate-resistant Chinese hamster ovary cell line. *Mol. Cell. Biol. 8*, 2316−2327.

Maniatis, T., Fritsch, E. F., & Sambrook, J. (1989) *Molecular cloning. A Laboratory Manual*, Cold Spring Harbor Laboratory, Cold Spring Harbor, NY.

McGhee, J. D., & Felsenfeld, G. (1979) Reaction of nucleosome DNA with dimethyl sulfate. *Proc. Natl. Acad. Sci. U.S.A. 76*, 2133−2137.

McGrogan, M., Simonsen, C. C., Smouse, D. T., Farnham, P. J., & Schimke, R. T. (1985) Heterogeneity at the 5′ termini of mouse dihydrofolate reductase mRNAs. Evidence for multiple promoter regions. *J. Biol. Chem. 260*, 2307−2314.

Means, A. L., & Farnham, P. J. (1990) Transcription initiation from the dihydrofolate reductase promoter is positioned by HIP1 binding at the initiation site. *Mol. Cell. Biol. 10*, 653−661.

Milbrandt, J. D., Heintz, N. H., White, W. C., Rothman, S. M., & Hamlin, J. L. (1981) Methotrexate-resistant Chinese hamster ovary cells have amplified a 135-kilobase-pair region that includes the dihydrofolate reductase gene. *Proc. Natl. Acad. Sci. U.S.A. 78*, 6043−6047.

Milbrandt, J. D., Azizkhan, J. C., Greisen, K. S., & Hamlin, J. L. (1983) Organization of a Chinese hamster ovary dihydrofolate reductase gene identified by phenotypic rescue. *Mol. Cell. Biol. 3*, 1266−1273.

Mirzabekov, A. D., San'ko, D. F., Kolchinsky, A. M., & Melnikova, A. F. (1977) Protein arrangement in the DNA grooves in chromatin and nucleoprotamine *in vitro* and *in vivo* revealed by methylation. *Eur. J. Biochem. 75*, 379−389.

Mirzabekov, A. D., Bavykin, S. G., Belyavsky, A. V., Kharpov, V. L., Preobrazhenskaya, O. V., Shick, V. V., & Ebralidse, K. K. (1989) Mapping DNA−protein interactions by cross-linking. *Methods Enzymol. 170*, 386−408.

Mitchell, P. J., Carothers, A. M., Han, J. H., Harding, J. D., Kas, E., Venolia, L., & Chasin, L. A. (1986) Multiple transcription start sites, DNase I-hypersensitive sites, and an opposite-strand exon in the 5′ region of the CHO dhfr gene. *Mol. Cell. Biol. 6*, 425−440.

Mueller, P. R., & Wold, B. (1989) In vivo footprinting of a muscle specific enhancer by ligation mediated PCR. *Science 246*, 780−786.

Nacheva, G. A., Guschin, D. Y., Preobrazhenskaya, O. V., Karpov, V. L., Ebralidse, K. K., & Mirzabekov, A. D. (1989) Change in the pattern of histone binding to DNA upon transcriptional activation. *Cell 58*, 27−36.

Nedospasov, S. A., & Georgiev, G. P. (1980) Non-random cleavage of SV40 DNA in the compact minichromosome and free in solution by micrococcal nuclease. *Biochem. Biophys. Res. Commun. 92*, 532−539.

Noll, M., & Kornberg, R. D. (1977) Action of Micrococcal nuclease on chromatin and the location histone H1. *J. Mol. Biol. 109*, 393−404.

Nunberg, J. H., Kaufman, R. J., Chang, A. C. Y., Cohen, S. N., & Schimke, R. T. (1980) Structure and genomic organization of the mouse dihydrofolate reductase gene. *Cell 19*, 355−364.

Reeves, R. (1984) Transcriptionally active chromatin. *Biochim. Biophys. Acta 782*, 343−393.

Rill, R. L., Nelson, D. A., Oosterhof, D. K., & Hozier, J. C. (1977) Structural repeat units of Chinese hamster ovary chromatin. Evidence for variations in repeat unit size in higher eukaryotes. *Nucleic Acids Res. 4*, 771−789.

Shimada, T., & Nienhuis, A. W. (1985) Only the promoter region of the constitutively expressed normal and amplified human

dihydrofolate reductase gene is DNase I hypersensitive and undermethylated. *J. Biol. Chem. 260*, 2468−2474.

Shimada, T., Inokuchi, K., & Nienhuis, A. W. (1986) Chromatin structure of the human dihydrofolate reductase gene promoter. Multiple protein-binding sites. *J. Biol. Chem. 261*, 1445−1452.

Shimada, T., Inokuchi, K., & Nienhuis, A. W. (1987) Site-specific demethylation and normal chromatin structure of the human dihydrofolate reductase gene promoter after transfection into CHO cells. *Mol. Cell. Biol. 7*, 2830−2837.

Shimada, T., Fujii, H., & Lin, H. (1989) A 165-base pair sequence between the dihydrofolate reductase gene and the divergently transcribed upstream gene is sufficient for bidirectional transcriptional activity. *J. Biol. Chem. 264*, 20171−20174.

Sigman, D. S. (1990) Chemical nucleases. *Biochemistry 29*, 9097−9105.

Simpson, R. T. (1991) Nucleosome positioning: occurrence, mechanisms, and functional consequences. *Prog. Nucleic Acids Res. Mol. Biol. 40*, 143−184.

Smith, M. L., Mitchell, P. J., & Crouse, G. F. (1990) Analysis of the mouse Dhfr/Rep-3 major promoter region by using linker-scanning and internal deletion mutations and DNase I footprinting. *Mol. Cell. Biol. 10*, 6003−6012.

Smith, P. A., Jackson, V., & Chalkley, R. (1984) Two-stage maturation process for newly replicated chromatin. *Biochemistry 23*, 1576−1581.

Tazi, J., & Bird, A. (1990) Alternative chromatin structure at CpG islands. *Cell 60*, 909−920.

Thoma, F. (1988) Mechanisms of nucleosome positioning tested in minichromosomes of yeast Saccharomyces cerevisiae. In *Architecture of eukaryotic genes* (Kahl, G., Ed.) pp 269−280, VCH Verlagsgesellschaft MBH, D-6940, Weinheim.

Thoma, F., & Zatchej, M. (1988) Chromatin folding modulates nucleosome positioning in yeast minichromosomes. *Cell 55*, 945−953.

Travers, A. A. (1989) DNA conformation and protein binding. *Annu. Rev. Biochem. 58*, 427−452.

Tullius, T. D., Dombroski, B. A., Churchill, M. E. A., & Kam, L. (1987) Hydroxyl radical footprinting: a high-resolution method for mapping protein−DNA contacts. *Methods Enzymol. 155*, 537−558.

Widmer, R. M., Lezzi, M., & Koller, T. (1987) Structural transition in inactive Balbiani ring chromatin of Chironomus during micrococcus nuclease digestion. *EMBO J. 6*, 743−748.

Wu, C. (1980) The 5′-end of Drosophila heat shock genes in chromatin are hypersensitive to DNase I. *Nature 286*, 854−860.

Wu, R. S., Panusz, H. T., Hatch, C. L., & Bonner, W. M. (1986) Histones and their modifications. *CRC Crit. Rev. Biochem. 20*, 201−263.

Yang, J. K., Masters, J. N., & Attardi, G. (1984) Human dihydrofolate reductase gene organization. Extensive conservation of the G + C-rich 5′ non-coding sequence and strong intron size divergence from homologous mammalian genes. *J. Mol. Biol. 176*, 169−187.

Yaniv, M., & Cereghini, S. (1986) Structure of transcriptionally active chromatin. *CRC Crit. Rev. Biochem. 21*, 1−26.

BI941845O